Cost Update: Commercial and Advanced Heliostat Collectors

Parthiv Kurup, Sertaç Akar, Stephen Glynn, Chad Augustine, and Patrick Davenport

National Renewable Energy Laboratory

NREL is a national laboratory of the U.S. Department of Energy
Office of Energy Efficiency & Renewable Energy
Operated by the Alliance for Sustainable Energy, LLC

This report is available at no cost from the National Renewable Energy Laboratory (NREL) at www.nrel.gov/publications.

Contract No. DE-AC36-08GO28308

Technical Report
NREL/TP-7A40-80482
February 2022

Cost Update: Commercial and Advanced Heliostat Collectors

Parthiv Kurup, Sertaç Akar, Stephen Glynn, Chad Augustine, and Patrick Davenport

National Renewable Energy Laboratory

Suggested Citation
Kurup Parthiv, Sertaç Akar, Stephen Glynn, Chad Augustine, and Patrick Davenport. *Cost Update: Commercial and Advanced Heliostat Collectors*. Golden, CO: National Renewable Energy Laboratory. NREL/TP-7A40-80482. https://www.nrel.gov/docs/fy22osti/80482.pdf.

NREL is a national laboratory of the U.S. Department of Energy
Office of Energy Efficiency & Renewable Energy
Operated by the Alliance for Sustainable Energy, LLC

This report is available at no cost from the National Renewable Energy Laboratory (NREL) at www.nrel.gov/publications.

Contract No. DE-AC36-08GO28308

Technical Report
NREL/TP-7A40-80482
February 2022

National Renewable Energy Laboratory
15013 Denver West Parkway
Golden, CO 80401
303-275-3000 • www.nrel.gov

NOTICE

This work was authored by the National Renewable Energy Laboratory, operated by Alliance for Sustainable Energy, LLC, for the U.S. Department of Energy (DOE) under Contract No. DE-AC36-08GO28308. Funding provided by U.S. Department of Energy Office of Energy Efficiency and Renewable Energy Solar Energy Technologies Office. The views expressed herein do not necessarily represent the views of the DOE or the U.S. Government.

Acknowledgments

The authors wish to thank the Concentrating Solar Power Subprogram of the U.S. Department of Energy Solar Energy Technologies Office for program support, and Solar Dynamics LLC and Schlaich Bergermann und Partner, sbp sonne GmbH (sbp) for communications, data, and insights related to their heliostat designs. The depth of analysis would not have been possible without such valuable contribution. This work was supported by the U.S. Department of Energy under Contract No. DE-AC36-08GO28308 with the National Renewable Energy Laboratory.

Acronyms

BOM	bill of materials
CAD	computer-aided design
CAPEX	capital expenditure
CSP	concentrating solar power
DFA	Design for Assembly
DFM	Design for Manufacturing
DFMA	Design for Manufacturing and Assembly
DLR	Deutsches Zentrum für Luft- und Raumfahrt (German Aerospace Center)
DNI	direct normal irradiance
DOE	U.S. Department of Energy
GW	gigawatt
hrs	hours
HTF	heat transfer fluid
ITC	investment tax credit
kPa	kilopascal
kW_e	kilowatts electric
kWh	kilowatt-hours
kWh_{th}	kilowatt-hours thermal
lbs	pounds
LCOE	levelized cost of energy
MW_e	megawatt (electric)
NREL	National Renewable Energy Laboratory
ROP	ring of power
SAM	System Advisor Model
sbp	Schlaich Bergermann und Partner, sbp sonne GmbH
SMEs	small and medium enterprises
TES	thermal energy storage
USD	U.S. dollars
yrs	years

Executive Summary

The research team performed a detailed bottom-up manufacturing cost estimate for two heliostat designs: (1) a commercial design, the Stellio and (2) an advanced/developing heliostat design, the SunRing. The SunRing is designed and developed by Solar Dynamics of the United States, and the Stellio is developed primarily by Schlaich Bergermann und Partner (sbp) sonne GmbH. The Stellio heliostat has been deployed at commercial scale and is being used at the 50-megawatt electric (MW_e) Hami Concentrating Solar Power (CSP) power tower plant in China. For both designs, the bottom-up manufacturing cost estimates included all components for manufacturing and assembly in a manufacturing facility (e.g., struts and frame) using Design for Manufacturing and Assembly (DFMA) software, and the purchased parts (e.g., mirrors, control systems, and drives). The field-assembly and construction activities were also considered to determine the installed cost of the modeled solar fields.

In both cases, the modeled heliostat field area was approximately 1.1 million square meters (Mm^2) in total solar field aperture area, which is the solar field area needed for a CSP baseload power tower plant. This modeled ~1.1 Mm^2 solar field is suited for an 80- MW_e CSP power tower plant with 12–16 hours (hrs) of thermal energy storage based on system advisor model (SAM) analysis. The land area for the modeling was approximately 1 square mile. For the Stellio solar field of 1,078,592 m^2 that was comprised of 22,239 heliostats, the estimated installed cost was \$127/m^2. The installed cost included the manufacturing cost, the purchased components, and installation. The SunRing analysis estimated the installed cost of 40,000 heliostats with 1,078,560 m^2 of aperture area to be approximately \$96/m^2.

In the System Advisor Model version used in this study (SAM 2020.11.29), the value of the installed cost of the heliostat field was \$140/m^2 for a commercial heliostat. The updated installed heliostat solar field costs for a ~1.1 Mm^2 heliostat field are \$127/m^2 for the commercial design and \$96/m^2 for the advanced/developing design. The overall capital expenditures (CAPEX) amounted to approximately \$137.0 million for the commercial design and \$103.5 million for the advanced/developing design. Given the default solar field costs, these costs could lead to reductions of 9.3% and 31.5% respectively from a \$151.0-million solar field based on the \$140/m^2 default heliostat costs.

When SAM was used to estimate the impact of the levelized cost of electricity (LCOE) based on the CAPEX costs, including the 26% federal investment tax credit (ITC) available to CSP projects that start construction in 2021 or 2022, and using the default financial conditions, the LCOE was \$94.4/MWh for Tucson, Arizona. When the advanced and commercial heliostat costs were used with the same financial conditions, the LCOE could drop by 3% and 10% respectively (\$91.6/MWh and \$850/MWh). This study aims at estimating LCOE by using the updated CAPEX and default heliostat performance values in SAM. The model does not attempt to test or compare the actual optical performance of the Stellio or the SunRing collectors.

Table of Contents

List of Figures

List of Tables

1 Introduction

Concentrating solar power (CSP) technologies capture the heat of the sun to drive a thermo-electric power cycle, and they can provide process heat (Turchi et al., 2019). At present, the most widely deployed CSP technology for power generation uses parabolic trough collectors. As of 2020, of the 6,128 megawatt electric (MW_e) of worldwide installed operating CSP capacity, more than 4,000 MW_e utilize parabolic trough collectors (SolarPACES, 2020; Turchi et al., 2017). Power towers, the second-most deployed CSP technology, comprise nearly 2 gigawatts (GW) of global operating capacity (SolarPACES, 2020). Of the approximate 1.4 GW of CSP construction worldwide in 2020, 0.3 GW was for power towers (REN21, 2021). In the United States, as of 2021, 392 MW_e of power tower CSP capacity were operating at the Ivanpah Solar Electric Generating System in California (NREL, 2021); however, this capacity, which represents approximately 23% of the U.S. operating CSP capacity (NREL, 2020a; SolarPACES, 2020), is from direct steam generation rather than molten salt power towers.

The largest CSP plant being constructed in the world is the 700-MW_e combined parabolic trough and power tower system in Dubai, United Arab Emirates. The Dubai Electricity and Water Authority 700- MW_e complex is composed of 600 MW_e of parabolic troughs (i.e., 3 x 200 MW_e trough plants) and a 100- MW_e molten salt tower site, with each plant having 12–15 hours of thermal energy storage (TES) (Lilliestam and Pitz-Paal, 2018; SolarPACES, 2019). At present, the largest operating power tower plant in the world is a 150-MW_e plant with 7.5 hours of TES in Morocco (Chamberlain, 2019). In June 2021, a 110- MW_e molten salt power tower with 17.5 hours of TES in Chile was inaugurated (Business Wire, 2021).

Power tower plants have large arrays of mirrors called heliostats that focus sunlight onto a receiver at the top of a tower. Figure 1 (top panel), shows the 510-MW_e Noor Ouarzazate solar complex in Morocco, which includes two parabolic trough plants (Noor I and II, 160 MW_e and 200 MW_e respectively), and one molten salt power tower plant (Noor III, 150 MW_e) (Kraemer, 2018). Figure 1 (bottom panel) shows the heliostats focusing the light onto the Noor III receiver. Molten salt is the heat-transfer fluid (HTF) in most power towers cases. Solar salt, which is melted so that it is fluid, is a blend of potassium and sodium nitrate; it acts as the HTF and the heat storage for large CSP plants (SQM, 2018). The molten salt flows through the receiver and is heated by the absorbed sunlight. The hot fluid can then generate steam that turns a conventional steam turbine-generator to produce electricity. The spent steam from the turbine is condensed into water and recirculated by feedwater pumps to be transformed back into high-pressure steam.

Wet, dry, or hybrid cooling processes can be used to cool and condense the spent steam; the selection of a process will influence water consumption, cycle performance, and cost. CSP power tower plants, while predominantly they were wet-cooled in the past, are now mainly dry/air or hybrid cooled, for the water savings in sensitive arid environments (IRENA, 2016).

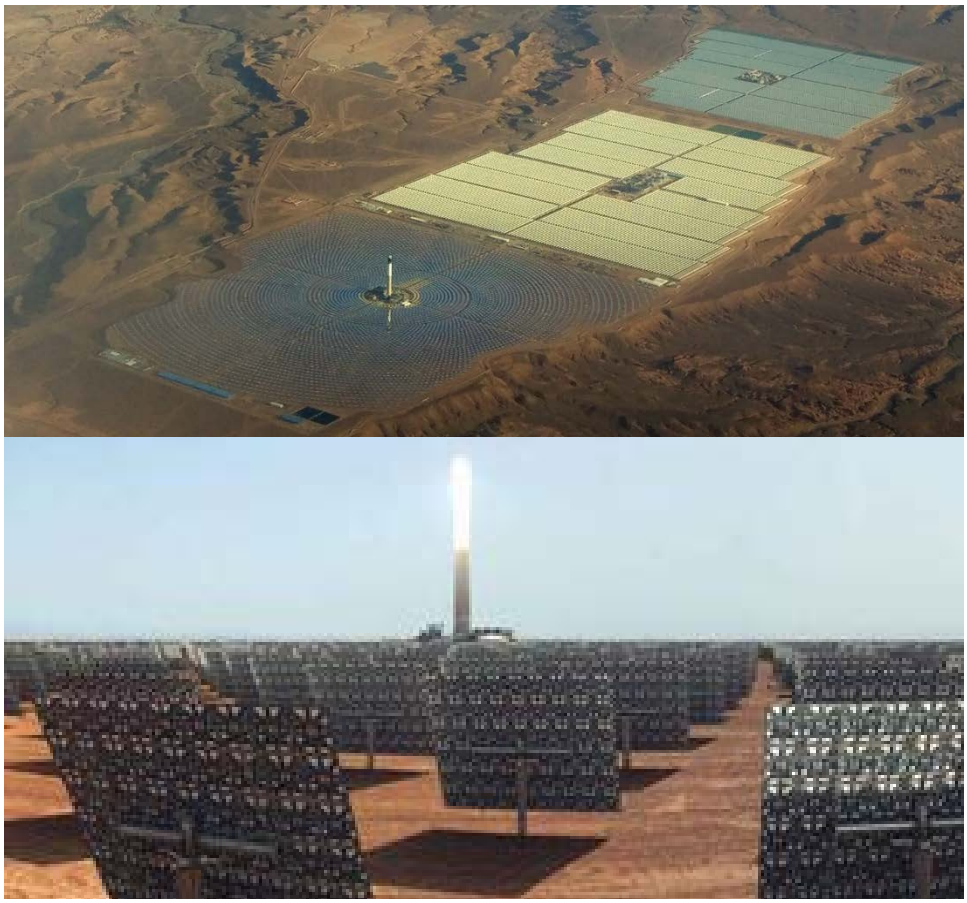

Figure 1. Noor Ouarzazate complex (top), and Noor III power tower plant (bottom), Morocco

Photos by courtesy of the engineering company SENER (2019)

A molten salt power tower plant is composed of the following subsystems: heliostat field, power tower and receiver, associated HTF and TES system, power block, fossil-fired backup (optional), and necessary ancillary facilities; see Figure 2. It shows a simplified molten salt power tower plant, without fossil fuel back-up and a two-tank TES—consisting of cold (290°C) and hot (565°C) tanks—that operates with a molten salt HTF (Dersch et al., 2019). The heat collected in the receiver is directly transferred to the two-tank TES, and an indirect heat exchanger is not needed unlike most parabolic trough plants, which use molten salt for the TES (IRENA, 2016).

All molten salt power tower plants currently operate with the latest generation of nitrate-based solar salts, which have an operating temperature limit of 565°C and have been proven in many molten salt power tower plants, such as Noor III. Noor III, which has been operating since December 2018, has exceeded performance expectations in ramp-up and regular operating situations; and long-term operations will be monitored and improved (Kraemer, 2019).

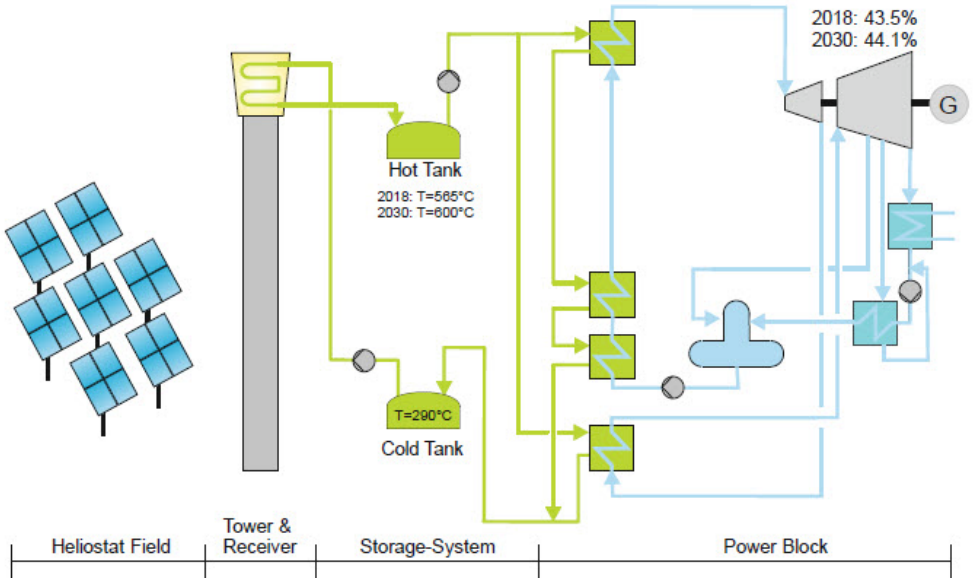

Figure 2. Simplified schematic of a stand-alone reference power tower plant in 2030

Illustration by the German Aerospace Center (Deutsches Zentrum für Luft- und Raumfahrt, or DLR)

Current molten salt is a binary blend of potassium and sodium nitrate, 40% and 60% by weight respectively (Dersch et al., 2019; SQM, 2018). DLR expects solar salts, with slightly higher operating temperatures of 600°C by 2030 and that these will lead to power block efficiency gains of 43.5%–44.1%, as shown in Figure 2 (Dersch et al., 2019).

The U.S. Department of Energy (DOE) is also pursuing higher temperatures to increase the power block efficiency of CSP. DOE is leading the development of next-generation CSP plants, called Gen3, with the goal of operating temperatures of 720°C as described in the report, *Concentrating Solar Power Gen3 Demonstration Roadmap* (Mehos et al., 2017). The Gen3 road map identified three potential receiver pathways, each using a different phase of matter—molten salt (liquid), particles (solid), or supercritical CO_2 (gaseous)—to collect and transport thermal energy from the receiver.

In March 2021, DOE selected the falling particle pathway as the most promising way to achieve Gen3 goals and awarded $25 million in federal funding to build an integrated falling particle CSP test facility (DOE EERE, 2021a). DOE is still funding efforts related to the molten salt and gas pathways, and researchers around the world are pursuing similar paths as well (Shultz, 2021). However, all three pathways use a solar field comprised of heliostats aimed at a central tower and use heliostats similar to those discussed in this report. Importantly, further improvement of heliostats (more than just cost reductions) are needed to achieve DOE's 2030 target of ¢5/kWh for CSP generation systems (Mehos et al., 2016). To meet the SunShot 2030 ¢5/kWh target, the installed cost of the heliostat field needs to be approximately $50/m^2 (Murphy et al., 2019).

2 Background and Motivation

2.1 Historical NREL Cost Analyses

In 2010, NREL established a baseline cost for parabolic trough technology in the United States by modeling and costing a 100- MW_e parabolic trough plant with 6 hours of TES (Turchi, 2010). The project was a joint undertaking of NREL and WorleyParsons Group. In 2015, NREL published a costing study of the SkyFuel SkyTrough and Flabeg's (technology now exclusively distributed by sbp Ultimate Trough parabolic trough collectors (Kurup and Turchi, 2015). The most recent detailed bottom-up manufacturing costing and installed cost analysis (Kurup et al., 2021) updated prior trough work and added the new Solar Dynamics SunBeam parabolic trough collector.

In 2013, NREL established a baseline for molten-salt power tower technology in the United States (Turchi and Heath, 2013). That study used Advanced Thermal Systems' older 148-m^2 heliostat design as documented by Kolb et al. (2007). This older heliostat design was also used as the baseline in DOE's 2010 Power Tower Roadmap (Kolb et al., 2011). In 2015, NREL provided DOE with an update to the estimated cost of a molten salt power tower that included a cost estimate for BrightSource Energy's LH-2.2 heliostat design that is deployed at the Ivanpah Solar Electric Generating System in California (Turchi et al., 2015).

The objective of this report is to provide detailed analysis of manufacturing, assembly, and construction costs for heliostats that lead to installed cost estimates for a commercial and an advanced heliostat field. Doing so is intended to update the assumed baseline costs for heliostat solar fields in the United States, similar to the work done in NREL's 2020 parabolic trough study (Kurup et al., 2021). The analysis considers both current and next generation heliostats, which we refer to as commercial and advanced heliostats respectively.

2.2 Selection of SunRing and Stellio Heliostats

Before selecting the Stellio and the SunRing for detailed analysis, we involved several heliostat developers and then down-selected technologies. In 2019 and 2020, we approached developers such as BrightSource Energy, Heliogen, and 24/7 Solar and prototype heliostat developers such as DLR about potentially participating in this analysis. Our selection of sbp's and Solar Dynamics' heliostats was secured with a strong collaborative approach with small and medium enterprises (SMEs), input from DOE and trust in NREL's capabilities, and the quality and level of data the companies were willing to share. During 2020 and 2021, we worked closely with Solar Dynamics' new advanced CSP heliostat design, the SunRing, and sbp's Stellio heliostat to undertake the analysis.

Stellio's heliostat design is characterized by a medium size (48.5 m^2) individual aperture area with a pentagon shape and backing by 10 cantilever arms, a central hub and an innovative kinematics with inclined axes driven by two linear actuators (Keck et al., 2019). The pentagon design leads to a more homogenous stiffness distribution than rectangular structures, and it results in a very efficient structural system. Five rings of purlins carry the mirrors, which are made from profiled sheet metal with cutting. The hub and the parts of the kinematic system are welded from plates. The whole structure is hot dip galvanized for corrosion protection. Ten mirror facets from 4-mm float glass and a central mirror form the 48.5 m^2 reflecting surface.

The mirrors are connected to the steel structure by a gluing process, in a high precision jig that provides an accurate mirror curvature without any adjustment (Keck et al., 2019). Stellio was originally developed for solar fields similar to the 100- MW_e Redstone plant in South Africa (Acwa Power, 2021).

Figure 3. Stellio heliostat field for the 50- MW_e molten salt solar tower project at Hami

Photo by sbp

The first commercial application of the Stellio heliostat is the 50- MW_e molten salt solar tower Hami project in the Xinjiang province near the China-Mongolia border (CSP Focus, 2020; Keck et al., 2019). Figure 3 shows the operating and installed Stellio field. Hami is a central receiver plant that uses molten salts as the HTF, has an aperture area of 703,250 m^2 with 14,500 heliostats, and is designed with an 8-hour TES (NREL and SolarPACES, 2021). It consists of the solar field and power block. The thermal efficiency of the power plant is 43%, assuming an ambient temperature 19°C. The back pressure of the air condenser is 8.5 kilopascals (kPa). The thermal efficiency of thermal storage and heat transfer system reaches 99% in operation (Keck et al., 2019). The predicted capacity of thermal storage is 1,430 MWh, which is enough to run the turbine at full output for 12 hours. The annual generated energy is 198.4 GWh (Keck et al., 2019; NREL and SolarPACES, 2021).

Solar Dynamic's SunRing Heliostat is an evolution of Abengoa's Ring of Power (ROP) design (Tilley et al., 2014). The ROP design was chosen based on a balance of cost, accuracy, and cost risk. Strong drivers in selecting the ROP's smaller size were its ability to minimize labor costs and the impact varying labor rates would have on the heliostat, which together enable a single heliostat design suitable for the worldwide CSP market. The ROP was a carousel type design in which loads were transmitted through a space frame down to the large azimuth drive ring, which enabled a small stepper motor to be used for the azimuth drive. The ROP eliminated the need for a central foundation by using a unique concrete ring foundation directly supporting the azimuth drive ring, which made for a compact package that could be assembled in one location and then transported for field installation.

Solar Dynamics improved on the ROP concept with their SunRing through an increase in aperture area, improved (patent-pending) structure arrangement and azimuth drive, a simpler facet design, and a robust foundation. With 27m^2 of flat, rectangular, mirrored aperture area, the SunRing is smaller than the Stellio. The mirrors are supported by simplified ribs that are connected to a large torque tube. The torque tube is supported by a space frame and linear actuator that creates the elevation drive. The space frame is connected to hubs, which house wheels that ride on a large-diameter tubular azimuth ring. Azimuth rotation is obtained through a DC motor driving a pinion engaging a gear welded to the azimuth ring. The SunRing foundation is connected to the azimuth ring directly, which eliminates the need for a large central pylon. The foundation can consist of three or more helical ground anchors (we modeled six in this study) or a concrete ring depending on soil conditions at a particular site. Similar to commercial heliostats, the SunRing has been designed to be constructed rapidly on-site in an assembly line fashion from subassemblies. Its smaller size enables it to be moved via a specially equipped telehandler to its location quickly with minimal labor.

Figure 4 shows the sbp Stellio and the Solar Dynamics SunRing heliostats. Unlike parabolic troughs, which connect modules into larger assemblies, the single module is the heliostat.

Figure 4. sbp Stellio heliostat (left), and Solar Dynamics SunRing heliostat (right)

Photos by sbp and Solar Dynamics

We considered only an available commercial design (i.e., the Stellio) and an advanced design (i.e., the SunRing). See Table 1 for details about each design.

Table 1. Commercial and Advanced Heliostats Examined in this Study

Property	Stellio	SunRing
Developer	sbp (Germany)	Solar Dynamics (USA)
Reflector type	4-mm glass	4-mm glass
Individual heliostat aperture (m^2)	48.5	26.964
Heliostats per field	22,239	40,000
Size of solar field (m^2)	1,078,592	1,078,560
Design geometry	Pentagonal	Rectangular
Design drive type	Linear actuators	Linear actuator, DC gearmotor
Primary frame material	Steel	Steel

3 Approach and Methodology

3.1 Key Assumptions and Limitations

Our aim for the SunRing and Stellio bottom-up costing was to create a representative case for the commercial and advanced designs at a scale suited for large heliostat fields. Many key assumptions were needed for both designs for our bottom-up cost modeling. We discuss the most important assumptions in this section.

For the solar fields modeled, we determined the mirror area in a good solar resource area would be sufficient for a CSP plant of 80 MW_e with 8 hours of TES. This field area is similar to those in prior analyses where the plant size was 90–100 MW_e (Kurup et al., 2021; Kurup and Turchi, 2015; Turchi, 2010), and the area is reasonably representative of current power tower projects. Note the focus of the analysis is the solar field size, and therefore the number of heliostats and the aperture area of the field, rather than the design of a specific solar field for a certain plant capacity or hours of storage.

The approximate solar field aperture area for each modeled heliostat field is 1.1 million m^2 (Mm^2). For a real plant, the aperture area would depend on the assumed solar multiple, location and associated direct normal irradiance (DNI) resource. The exact solar field size is not critical, but we did need to specify a size we could use for the production volume calculations within the Design for Manufacturing and Assembly (DFMA) software (Boothroyd Dewhurst Inc., 2020). The scope of this analysis relative to the cost categories within the System Advisor Model (SAM) is outlined in Table 2.

Table 2. SAM Heliostat Direct Capital Cost and Other Key Categories within SAM

Source: Turchi et al., 2019

SAM Direct Capital Cost Categories	SAM 2020
Solar field, which includes: • Solar collector mirrors • Solar collector fittings • Solar collector frame • Solar collector assembly misc. components e.g., rivets • Foundations and support structures • Instruments and controls • Electrical cabling • Installation labor • Assembly infrastructure: temporary building, jigs, cranes, etc.	$140/m^2$
Molten salt TES and HTF system, which includes: • Freeze-protection system • High-temperature HTF pumps • Foundations and support structures for the two tanks • Salt and inventory	$22.0/kWh_{th}$
Power cycle cost	$1,040/kW_e$
Balance of plant cost	$290/kW_e$

The following sections provide the estimates and breakdowns for the manufactured costs, assembly and field construction activities leading to an estimated installed cost per square meter of aperture area ($/m^2) of the SunRing and the Stellio heliostats.

The purchased components are key, and are also included based on vendor quotes, data exchange, and information provided by Solar Dynamics and sbp. Project-specific factors that may influence component pricing such as project size, project financing, and markups were excluded from the analysis. We estimate the cost of potential manufacturing, assembly within a manufacturing facility and then the purchased costs for commercial scales of the SunRing and the Stellio at approximately 1.1 Mm^2. The SunRing is ready for pilot scale deployment, and the sbp Stellio has reached commercial deployment (i.e., the Chinese Hami plant).

We assumed tooling investments would not be needed for standard manufactured components (e.g., angle brackets), and these tooling costs were only included where specific geometries or special parts were needed (e.g., stamped plates). Where necessary, investment in tooling was calculated and shown as a separate line item. The labor rate was calculated at $35/hr in Arizona, based on Bureau of Labor and Statistics rates and total compensation (BLS, 2020).

3.2 Method for Investigation

The method used to analyze the SunRing and the Stellio is shown in Figure 5. As noted in Figure 5, the geometry of some parts associated with the SunRing and Stellio required custom computer-aided design (CAD) models (e.g., Figure 6).

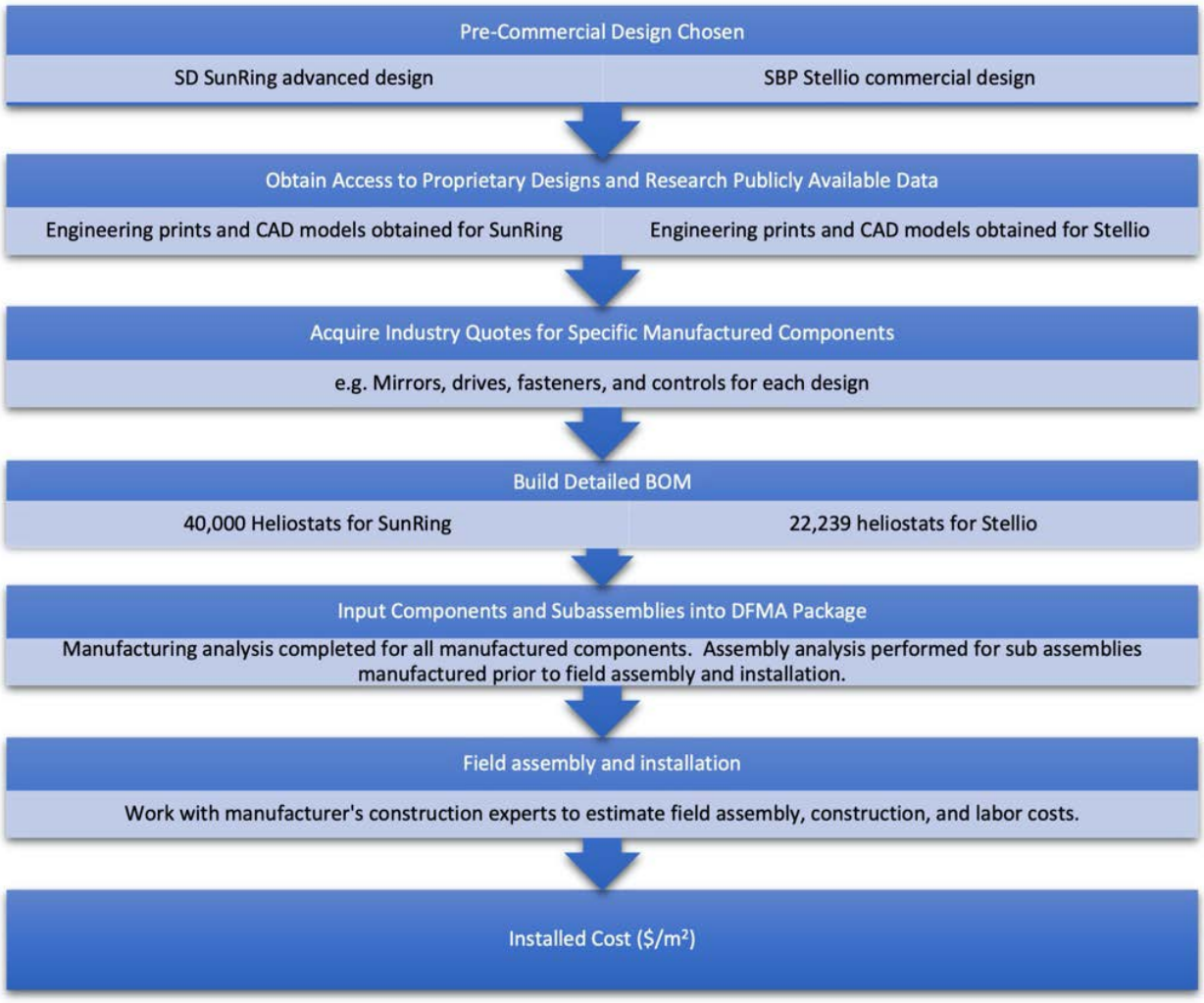

Figure 5. Method for determining the installed cost for the SunRing and Stellio heliostat designs

3.3 Bill of Materials Development

The development of an accurate bill of materials (BOM) is critical before DFMA can be performed, and a BOM underpins the bottom-up cost analysis. BOMs were developed from the drawings and CAD files provided by Solar Dynamics and sbp for the SunRing and Stellio heliostat designs respectively. Each design was broken into subassemblies that would be manufactured in a fabrication facility before being shipped to the site for field assembly and installation. Each subassembly consists of multiple components. All components were counted on a per Heliostat basis. The total number of components required for a given field size count could then be scaled by the number of heliostats required.

The components could be divided into manufactured components unique to a particular design and purchased components obtained from outside vendors. The volume of manufactured components and subassemblies could then be used as inputs to DFMA to capture the cost of manufacturing the volume of components (the life volume) needed for the representative solar field size.

3.4 Design for Manufacture and Assembly (DFMA) Software Package

A suite of Design for Manufacture and Assembly (DFMA) software tools from Boothroyd Dewhurst was a key tool in our analysis. This tool was used in a previous NREL CSP analysis from which the installed cost of a state-of-the-art commercial heliostat design was derived (Turchi et al., 2015), as well as the most recent bottom-up parabolic trough costing (Kurup et al., 2021). NREL has used DFMA in several other manufacturing cost analyses (Akar et al., 2018; Kurup et al., 2018; Mayyas and Mann, 2019; Van Geet et al., 2018).

The DFMA software package is used industry-wide and has two parts: Design for Manufacture (DFM) and Design for Assembly (DFA). For this analysis, the version of the DFM software was 4.0.2.208 and for the DFA software it was 10.3.2.208 (Boothroyd Dewhurst Inc., 2020). The DFMA tool has detailed databases and allows a knowledgeable user to calculate a primary manufacturing cost estimate for each component and then assemble it within the overall product/assembly.

We used DFM for most of the components within the BOMs to model the heliostat as if it were to be manufactured in commercial quantities needed for a large solar field. In this way, the material, manufacturing processes (e.g., stock processes), key dimensions, and machining steps were estimated. Note that not every component that could be directly manufactured in a commercial-scale manufacturing and fabrication shop was modeled because such specialist components such as linear actuators or mirror panels were beyond DFMA's capabilities. DFM allows the user to produce a detailed "should-cost" number that is based on what a component should cost from the manufacturer, specifically the material, process steps, machine setup time, and tooling if needed. Tooling investment is calculated for special processes such as stamping and also takes into account tool wear and life based on the life volume of the parts needed for the BOM.

We then used DFA used to assemble (e.g., weld) the components together into subassemblies and to cost the heliostat. We used DFMA for the heliostat structure and manufacturing estimates for the foundations. DFM can accept CAD models as inputs to allow the part to be modeled for manufacturing. For the SunRing and the Stellio BOMs, significant CAD models were needed because of the complexity of the parts, especially for certain components such as the strut connectors. An example of a CAD model of a SunRing actuator arm can be seen in Figure 6.

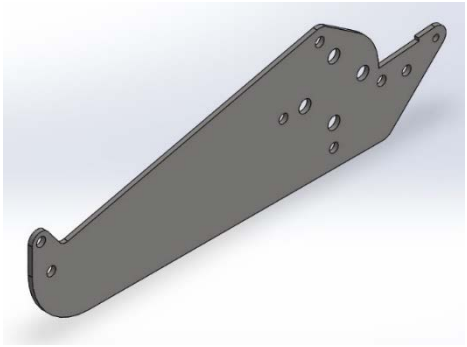

Figure 6. CAD model of a SunRing actuator arm plate used as input into DFM

Illustration by Solar Dynamics

A key feature of the DFMA tool is its built-in ability to change the life volume of the manufactured parts to compare the effects of small numbers of production and that of commercial-scale manufacturing. For example, increasing production volume from 8 to 80,000 for the component shown in Figure 6 caused the final manufactured part cost to drop from approximately $2,400/part for eight produced to approximately $10/part for 80,000 produced (which is marked by the vertical gray line intersecting the blue trace in Figure 7). This difference includes the tooling investment in the total part cost and the savings in the labor and material cost per part drives the inflection point.

Figure 7. Effects of manufacturing the SunRing actuator arm plate at various production scales

3.5 Interaction with Heliostat Developers

To build the bottom-up costing of the selected heliostat designs, significant interaction with the CSP industry was needed. For specific key components such as the silvered mirrors, control systems, and drive systems, price quotes were received from the component manufacturer or installer.[1] Details of the discussions and estimates provided by the industry are excluded from this report to protect the sensitive information provided. It must be stated that the cost estimates from suppliers and manufacturers used in this investigation were based on large-scale commercial application of the technology (e.g., enough for ~1,000,000 m^2 of aperture area). To determine the current market commodity prices of the steel (as raw materials and as manufactured parts), price indices for the commodities were created and used from the DFMA cost databases for U.S. materials. To note, prices may vary with the location of the manufacturing plant.

[1] Solar Dynamics and sbp were very supportive in providing this information. Without their support, the analysis would not have been possible at the level conducted.

4 Stellio Heliostat Design Analysis

4.1 Design Description

The Stellio heliostat is sized to ensure low effect of astigmatism to prevent optical losses or oversized receivers by using mirror elements that are designed for a standard float glass width of ~3.2 m. This medium size also allows usage of a central pedestal-based tracking design, and standard size drives and bearings (Balz et al., 2016). Each Stellio heliostat, as shown in Figure 8, has a pentagonal concentrator with reflective area of 48.5 m^2. A solar field with 22,239 heliostats represents a 1,078,592 m^2 of total aperture area, which is equivalent to the solar field size selected for the Solar Dynamics SunRing heliostats.

Figure 8. Stellio heliostats with mirrors cut of standard flat available glass panes

Photo by sbp

The Stellio heliostat uses linear drives for both axes that are enabled by a special axis arrangement that reduces the required angular ranges for both axes to ~110°, which is manageable with a linear actuator configuration. In addition, kinematics is selected in such a way that the linear drives are mostly tensile loaded; compressive forces happen only rarely and only when the drives are close to fully retracted; thus, buckling is not a problem, and slender cost-efficient drives can be used (Balz et al., 2016).

Stellio's rotationally symmetric, stiff structure is defined by a precise jig. Steel structure and mirrors are then connected by a special glue connection. On-axis canting is automatically achieved during assembly. Moreover, the number and location of mirror connection points (pads) has been optimized (Balz et al., 2016).

The Stellio local controller uses Arm Cortex-M4 processors (Balz et al., 2016). The software implemented contains forward kinematic and inverse kinematic models to represent deviations of heliostat axis orientation from the ideal orientation by evaluation of calibration shots on the tower target.

4.2 Subsystem Categories

The Stellio heliostat (Figure 9) is composed of subassemblies that include the foundation, cantilever arms, a central hub, mirrors (Inner Facet, Facet-1, and Facet-2), purlins (five sizes), the pylon base, the pylon head, a linear actuator, and the control system. Table 3 shows the subassembly and component number breakdown.

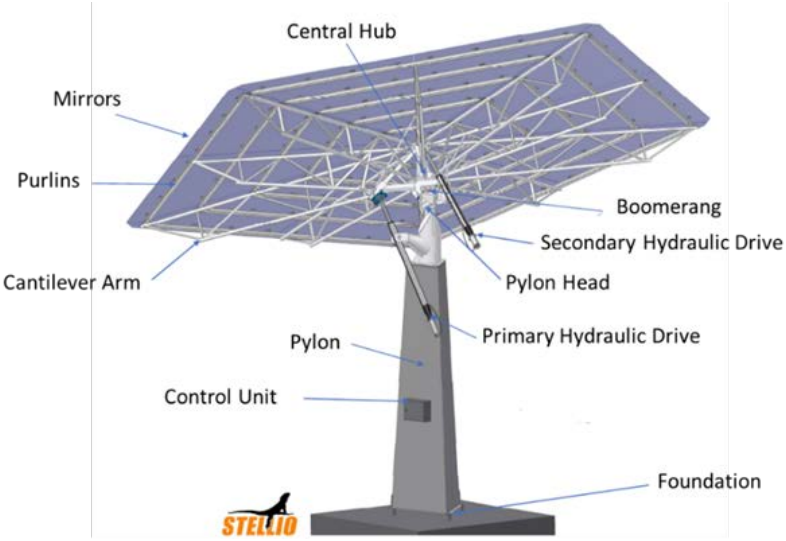

Figure 9. Schematics showing the main components of the sbp Stellio heliostat

Illustration by sbp

Table 3. Summary of the Individual Components per Subassembly for the Stellio Analysis

Subassembly	Discrete Components per Subassembly	Details
Cantilever arms	13	Five long and five short arms per heliostat; manufactured from nonalloy structural steel by cutting from stock with abrasive cutoff; compound die stamping used for can lug and can washer; assembled by welding
Central hub	23	Manufactured from low alloy hot rolled steel by using compound die stamping; assembled by welding
Boomerang	26	Manufactured from nonalloy structural steel using compound die stamping; assembled by welding
Pylon head	13	Manufactured from hot-dip galvanized steel using separate operations stamping, plasma cutting, compound die, computer numerical control lathe, and manual drill; assembled by welding
Pylon base (triangular)	21	Manufactured from hot-dip galvanized sheet steel using compound die, parted from coil stock of correct width, two parts per stroke, nested, and separate operations stamping, part off from coil of correct width; assembled by welding

4.3 Installed Cost for Heliostats

We performed our installed cost analysis of the Stellio heliostat for a production volume of 22,239 heliostats, which represents a solar field aperture area of 1,078,592 m^2. Site assembly and construction cost data was provided by sbp and adapted for the modeled solar field size. These costs include the equipment, infrastructure, and labor required to assemble and install all heliostats, each with an individual aperture area of 48.5 m^2 per heliostat. Our analysis yielded an installed cost of approximately \$127/m^2, and the breakdown can be seen in Figure 10. The \$127/m^2 includes a \$878,000 for tooling amortized over the production of the components and the tool life. For a field size of approximately 1.1 Mm^2, a \$7.5-million heliostat assembly facility adjacent to the solar field was also estimated. The total heliostat installed field CAPEX would be approximately \$136.98 million for the solar field. Based on detailed reviewed of the analysis with sbp, we concluded the estimate is within ±10% of the developer's own estimates for bids and projects.

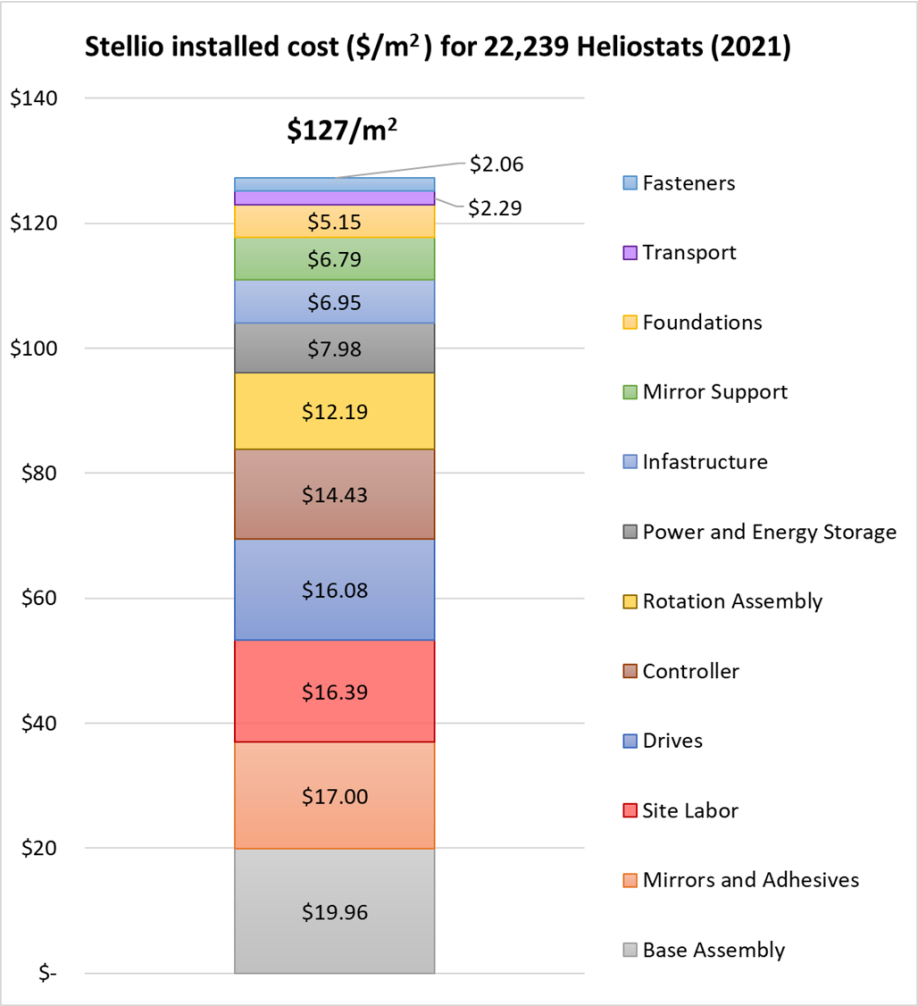

Figure 10. Installed cost for the Stellio assuming 22,239 heliostats yielding 1,078,592 m^2 of aperture area

Total installed cost is estimated at \$127/m^2.
Chart by Stephen Glynn and Sertac Akar, NREL

The largest contributors to the installed cost are the base assembly (15.68%) and mirrors (13.36%). The site labor costs (12.88%) represent the total expected labor costs required to assemble and install. After mirrors, the linear actuators (12.63%) and the control systems (11.34%) are the second-most important cost contributors as purchased parts. The other manufactured parts, which are rotation assembly (9.58%) and mirror support structure (5.33%), constitute 16% of the total installed cost. The foundation costs (4.05%) are variable because of site-specific considerations such as soil quality and expected wind loads. The transportation and shipping costs (1.80%) are based on domestic shipping within the United States and are calculated based on percentages of vendor quotes provided by sbp.

All other categories, including site infrastructure and assembly, electrical cabling, interconnections, and fasteners contribute 13.35% to the total installed cost. The fasteners category alone is a relatively large contribution, even after switching from traditional bolting or welding to riveted construction to reduce assembly time and costs at this manufacturing scale. This detail demonstrates the importance of each component and step in the manufacturing process. The Stellio heliostat uses a balance of purchased components and manufactured components, and a breakdown of the total cost by category is presented in Figure 11.

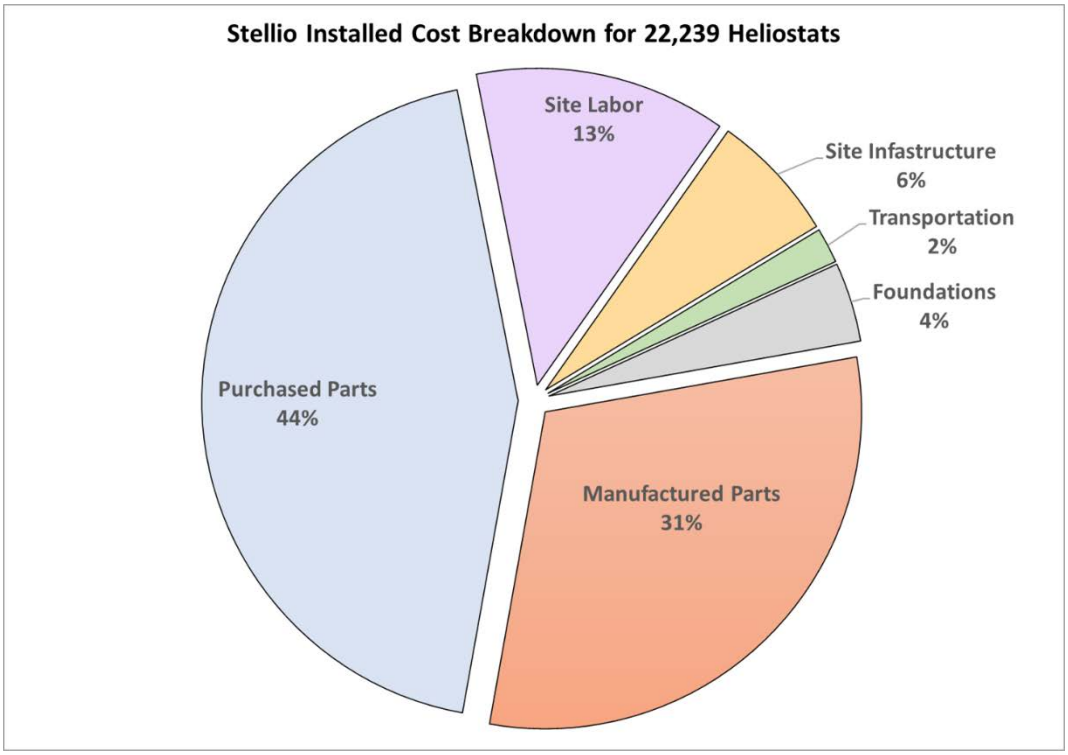

Figure 11 Total installed cost breakdown by category for sbp Stellio heliostat

Chart by Stephen Glynn and Sertac Akar, NREL

Purchased parts are the largest contributor to the total installed cost (44%). Manufactured parts and their fabrication into subassemblies that are shipped to the field (31%) are the second-largest cost contributors. Site labor (13%) and site assembly and fixtures (6%) are the third. The cost of foundations is 4%, and the cost of transportation/shipping is 2% of the total installed cost.

5 SunRing Heliostat Design Analysis

5.1 Design Description

Solar Dynamics's SunRing heliostat is an advanced and developing heliostat design that is an evolution of the Ring of Power (ROP) concept developed by Abengoa. It uses six 1.4 m x 3.21 m mirror facets in a canted configuration. Drives facilitate rotation of the heliostat about its base (azimuth) and alter the angle of the mirrors relative to the base (elevation). The SunRing is being tested at the stage of functional prototypes. Solar Dynamics's first-generation prototype is currently deployed the Solar Technology Acceleration Center in Colorado, and a second-generation prototype is currently in procurement.[2]

Figure 12. Rear view of the SunRing heliostat at the Solar Technology Acceleration Center, showing the pilings, base, drives, and mirror support structure

Photo by Kyle Kattke, Solar Dynamics

Our SunRing BOM was undertaken for a plant comprised of 40,000 heliostats. Each individual heliostat has a reflective area of 26.9 m^2, which yields a total field reflective area of 1,078,560 m^2. The power tower, molten salt, and turbine costs were excluded.

5.2 Subassembly Categories

The SunRing heliostat is composed of the subassemblies depicted in Figure 13. Ground anchors and mounts bolt to the geared azimuth ring. The base assembly has wheeled hubs that ride on the circular tube of the azimuth ring, and its rotation about the ring is controlled by a roller pinion that engages the azimuth gear. The lower structure forms the triangulated frame between the base assembly and the mirror support structure. The mirror support structure consists of two tubes with a series of brackets welded to them. The brackets allow for bolting of the mirror ribs to the mirror support structure and create the mounting points for the pivot to the lower support structure and linear actuator that controls the elevation angle of the mirrors. The mirrors are adhered to the mirror ribs. Adjacent to the mirrors is a small PV panel that is used to provide power the heliostat controls and drives.

[2] This prototype is the third generation of Abengoa's design.

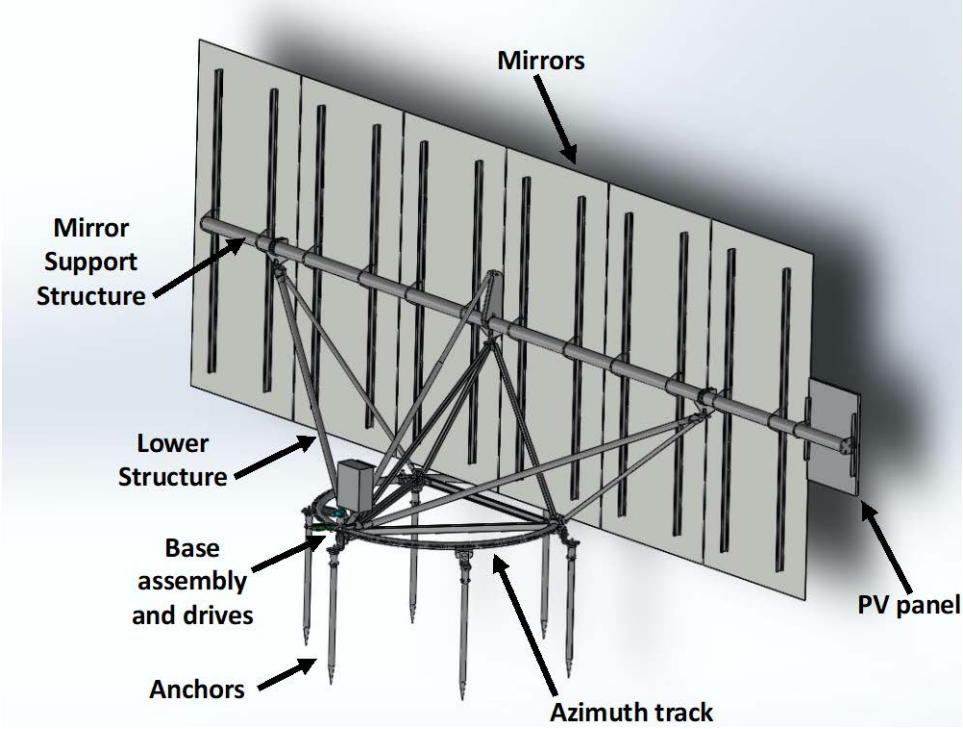

Figure 13. Rendering of SunRing heliostat shown from behind mirrors

CAD model drawing by Solar Dynamics. Image by Stephen Glynn, NREL, based on CAD model drawing by Solar Dynamics.

For each subassembly, we assessed engineering drawings and CAD models provided by Solar Dynamics. The drawings and models allowed for precise input of the dimensions, tolerances, and material specifications into DFM and DFA. The subassemblies were broken down into individual components for cost modeling within DFM. Subsequently, the components were assembled into their respective subassemblies within DFA.

Each heliostat is composed of 522 total parts, including all the fasteners. Of the 522 parts, 125 are unique. There are 52 discrete component designs manufactured specifically for a heliostat. Table 4 summarizes the major unique component breakdown of each subassembly while omitting the fasteners. These component designs were modeled in DFM and then assembled in DFA. Most of the parts are made of low-carbon structural steel and are galvanized after being made into subassemblies. Many of the parts were designed with high-volume manufacturing in mind, allowing for the utilization of stamping processes. The components and subassemblies were modeled at the appropriate volumes to assemble 40,000 heliostats. For example, six identical gear segments make up the azimuth gear track; therefore, the gear segment was modeled for a volume of 240,000 units.

The purchased component costs were from vendor estimates and were based on the scale of the field installation. The mirrors, fasteners, bushings, rollers, axles, battery, PV panel, drives and controllers were all purchased components.

Table 4. Summary of Individual Components per Subassembly for the SunRing Analysis

Subassembly	Discrete Components per Subassembly	Details
Geared azimuth track	5	Galvanized steel ring from tubing with gear segments, and tabs
Base assembly	20	Galvanized steel structure to ride on azimuth track
Mirror support structure	14	Galvanized tubes, with mounting plates, ribs and brackets
Lower structure assembly	10	Galvanized steel tubular and formed cross sections connecting the base assembly to the mirror support structure
Anchors and mount assembly	4	Mounting assembly and screw piles
Mirror panels	6	4-mm silvered glass
Power, controls, and storage	5	PV panel, battery, controller, wiring, and connectors
Drives	3	Linear actuators and encoders

5.3 Installed Cost for Heliostats

Our installed cost analysis of the SunRing heliostat was performed for a production volume of 40,000 heliostats, which represents a plant size of 80-MW_e with 12–16 hrs of TES. Site assembly and construction cost data was provided by Solar Dynamics. These costs include the equipment, infrastructure, and labor required to assemble and install all 40,000 heliostats. Arizona labor rates were used in this analysis.

With a total area of 26.96 m2 per heliostat, our analysis yielded manufactured and installed cost of approximately $96/m2. This includes a tooling investment (e.g., dies and stamping sections) of $450,000 and an assembly facility ($880,000). Both are amortized over the required production volume for 40,000 heliostats. The SunRing assembly facility consists of five stations that build the entire heliostat without the foundation in a common location. This can allow for heliostats to be completed every 7 minutes (Kattke, 2019). The heliostat is then transported to its final location using a single piece of heavy equipment. Based on a detailed review of the analysis with Solar Dynamics, we concluded the estimate is within ±5% of commercial cost forecasts developed internally by Solar Dynamics.

The total heliostat installed field CAPEX would be approximately $103.53 million, for 1,078,560 m^2 of aperture area. The tooling cost only accounts for $0.42/$m^2$ of the total cost. A breakdown of the total cost by category can be seen in Figure 14.

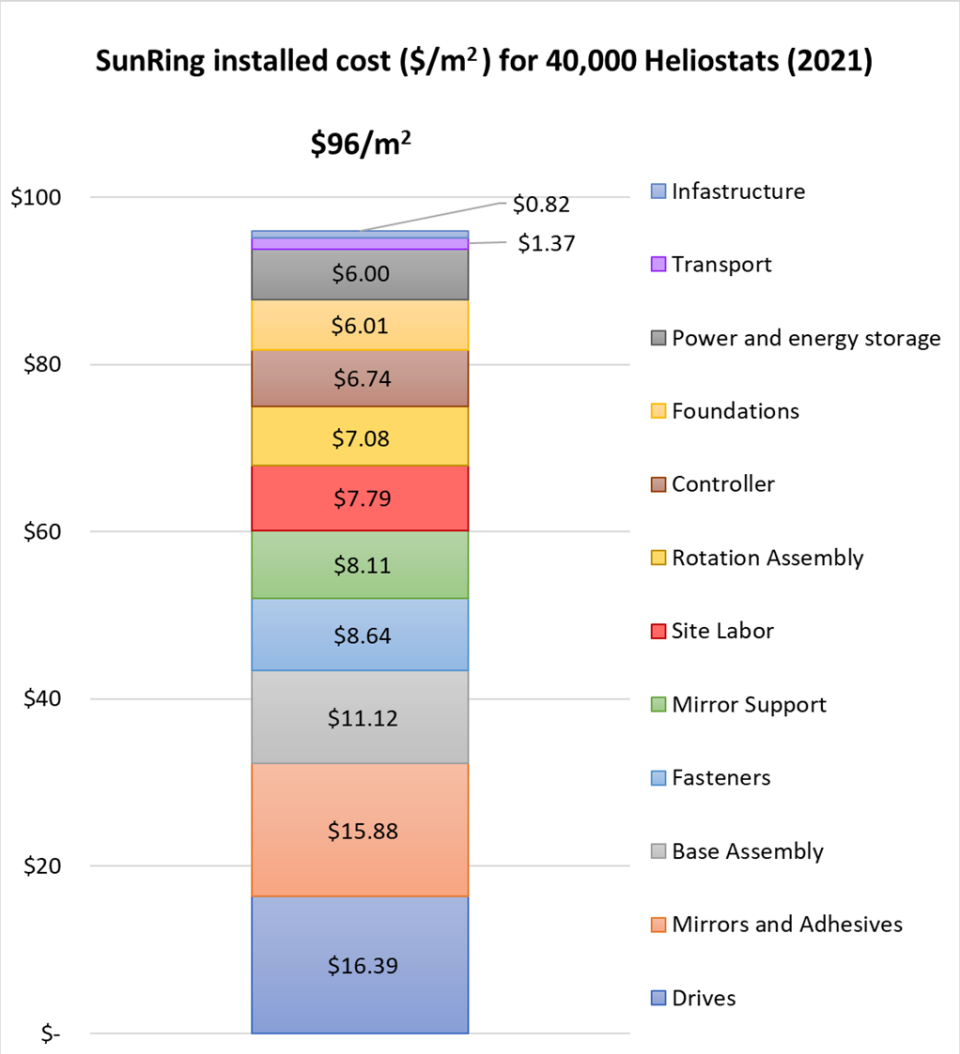

Figure 14 Installed cost for the SunRing assuming 40,000 Heliostats yielding 1,078,560 m² of aperture area

Total installed cost is estimated at $96/m².

Chart by Stephen Glynn and Sertac Akar, NREL

Figure 15 illustrates that the major cost drivers in the SunRing heliostat design are purchased components. The purchased components are 56% of the total cost. The drives and the mirrors account for almost one-third of the total cost. Manufactured components are 27% of the total cost. The base assembly is the largest cost of the manufactured subassemblies. This is because of both the large number of components within the base assembly and the mass and complexity of the hubs which ride on the azimuth track. The foundations can also be considered mostly purchased components, as the screw piles are 77% of that total cost. The fasteners, which include nuts, bolts, bushings, and rollers required for the assembly, are also a significant contribution. The mirror support structure is the second-largest manufactured subassembly contribution because of the mass and number of parts comprising it. The site labor and infrastructure account for only 8% and 1% of the total cost respectively.

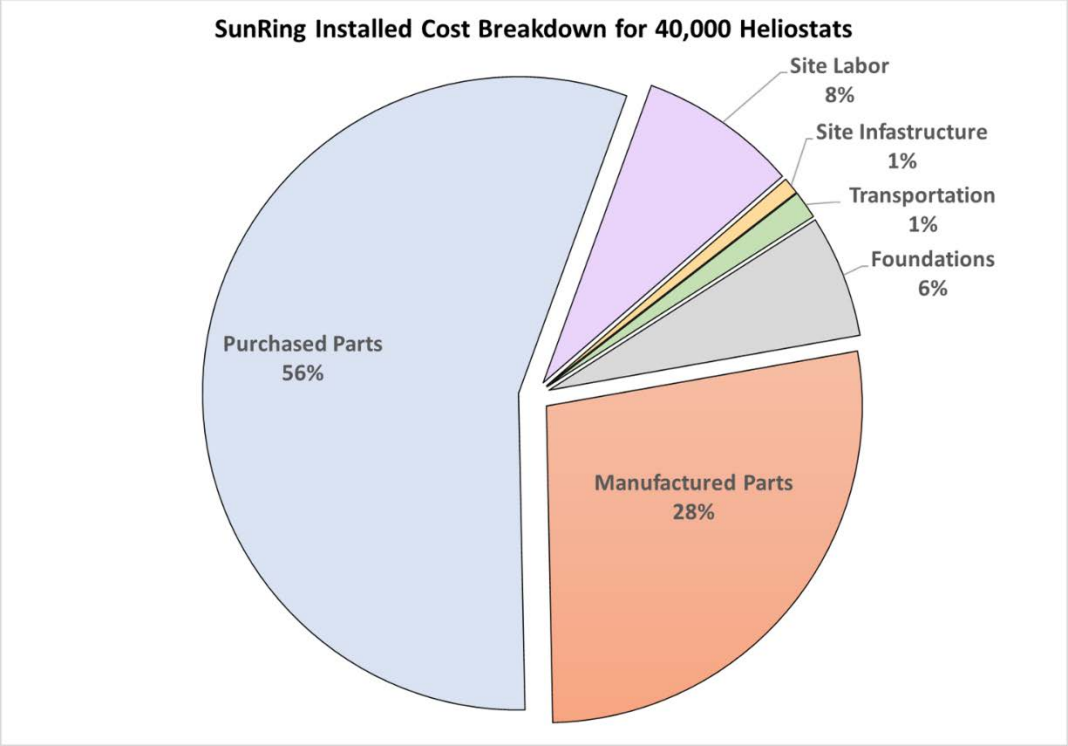

Figure 15 Total installed cost breakdown by category for Solar Dynamics SunRing heliostat

Chart by Stephen Glynn and Sertac Akar, NREL

6 Comparison of LCOE Estimates

In the current released version of SAM (2020.11.29) (NREL, 2020b), the default heliostat installed cost is \$140/m^2 for today's deployed heliostat. The \$140/m^2 was determined through analysis of the global CSP market, deployed projects, and a prior industrial survey (Turchi et al., 2019). To ascertain the impact of the heliostat cost on the overall plant cost and LCOE, we created a SAM simulation with three scenarios: Default heliostat (current cost), Commercial heliostat (sbp cost), and Advanced heliostat (SunRing cost). To allow for comparison, the three scenarios use the prebuilt heliostat aperture area (i.e., 144.4 m^2 in Table 5). Note, the number of heliostats for the Commercial and Advanced cost scenarios (22,237 and 39,944 respectively) are provided for reference if the aperture area were to be similar to the Default scenario in Table 5 and Table 6 (page 23); these numbers were not used in the SAM scenarios.

Table 5. Default, Commercial, and Advanced Heliostat CAPEX Cost Scenarios (*default is the current cost at SAM, commercial is the sbp cost, and advanced is the SunRing cost*).

Solar Field Category	Default Heliostat	Commercial Heliostat	Advanced Heliostat
Site improvements (\$/m2)	16	16	16
Individual heliostat aperture area (m^2)	144.4	48.5	27.0
Number of heliostats for similar sized field	7,470	22,237	39,944
Solar field size for similar fields (m^2)	1,078,480	1,078,495	1,078,488
Individual heliostat aperture area (m^2) used in scenario	144.4	144.4	144.4
Number of heliostats used for in the scenario	7,470	7,470	7,470
Solar field installed cost (\$/m^2) for scenario	140	127	96
Total installed heliostat field cost (\$)	\$151.0 million	\$137.0 million	\$103.5 million
Potential decrease in overall solar field CAPEX (%)	0%	-9.3%	-31.5%

The three SAM scenarios model the same 7,470 heliostats with an aperture area of 1,078,480 m^2 and varying only the installed cost from \$140/m^2 to \$127/m^2 and \$96/m^2. The installed cost is reflective of reflects the Commercial and Advanced costs determined in the bottom-up analysis. As highlighted in Table 5, the specific heliostat aperture area for the Commercial and Advanced heliostats (48.5 m^2 and 27 m^2) have not been used in the SAM scenarios; this is because SAM cannot model the Commercial and Advanced heliostats. The simulations in all three scenarios do not take optical performance of the commercial and advanced heliostat designs into account. As seen in Table 5, the total CAPEX for the installed heliostat fields was approximately \$151.0 million for the current default, \$137.0 million for the Commercial heliostat case, and \$103.5 million for the advanced heliostat scenario. As can be seen, the Commercial and Advanced

heliostat fields could reduce the overall solar field cost by 9.3% and 31.5% relative to the default cost in SAM 2020.11.29.

Table 6 highlights the other key cost categories (e.g., HTF and TES cost, power plant, and balance-of-plant costs), and financial parameters used for the techno-economic analysis in the SAM cases. For the techno-economic analysis and SAM scenarios, Tucson, Arizona (Location 1) and Daggett, California (Location 2) were used to highlight the impact of the location and DNI. To note, the labor values for the detailed manufacturing analysis were for Arizona. For the SAM analysis and scenarios, the installed solar field cost in California was assumed to be the same as in Arizona; this was inaccurate, as the labor rates are higher in California than Arizona. As highlighted, Arizona labor rates were used for the manufacturing cost and construction analysis. The analysis in Table 6 includes Location 2 (Daggett, California), as Daggett has excellent DNI and weather conditions, and so was used to highlight the impact of excellent DNI and the costs for a CSP plant in the three scenarios.

Table 6. Default, Commercial, and Advanced Cost Cases in SAM and the Impact on LCOE

SAM System Cost Category	Default Heliostat	Commercial Heliostat	Advanced Heliostat
Location			
Location 1	Tucson, Arizona	Tucson, Arizona	Tucson, Arizona
Annual generation (GWh) at Location 1	396.844	396.844	396.844
Location 2	Daggett, California	Daggett, California	Daggett, California
Annual generation (GWh) at Location 2	409.423	409.423	409.423
Heliostat Field			
Solar field installed cost ($/m^2)	140	127	96
Individual heliostat aperture area (m^2)	7,470	7,470	7,470
Number of heliostats	1,078,480	1,078,480	1,078,480
Total installed heliostat cost	$151.0 million	$137.0 million	$103.5 million
Tower and Receiver			
Tower ($)	20.9 million	20.9 million	20.9 million
Receiver ($)	60.9 million	60.9 million	60.9 million
Thermal Energy Storage			
TES cost ($/kWhth)	22.0	22.0	22.0
TES total cost ($)	34.2 million	34.2 million	34.2 million
Power Cycle			
Gross power block (MW$_e$)	80	80	80
Power cycle cost ($/kWe)	1,040	1,040	1,040
Balance-of-plant cost ($/kW$_e$)	290	290	290

SAM System Cost Category	Default Heliostat	Commercial Heliostat	Advanced Heliostat
Other Cost Categories for Locations 1 and 2			
Contingency on direct CAPEX (7% default, $)	27.3 million	26.3 million	24.0 million
Indirect: Engineering procurement and construction cost and owner costs ($)	54.3 million	52.3 million	47.7 million
Indirect: Total land cost ($)	9.5 million	9.5 million	9.5 million
O&M fixed cost by capacity ($/kW$_e$-yr)	66	66	66
Total Direct Costs for Location 1 and 2	$498.2 million	$480.7 million	$367.0 million
Total Installed Costs for Location 1 and 2 ($/kW)	6,920	6,676	6,095
Finance Assumptions			
Analysis period (years)	25	25	25
SAM LCOE real for Tucson, Arizona (¢/kWh)—without investment tax credit (ITC)	11.83	11.47	10.61
SAM LCOE real for Tucson, Arizona (¢/kWh)—ITC at 26% (DOE EERE, 2021b; SEIA, 2021)	9.44	9.16	8.50
SAM LCOE real for Daggett, California (¢/kWh)—without ITC	11.48	11.13	10.29
SAM LCOE real for Daggett, California (¢/kWh)—ITC at 26% (DOE EERE, 2021b; SEIA, 2021)	9.16	8.89	8.25

Table 6 shows the results of the SAM cases with the Default, Commercial, and Advanced costs, assuming the remainder of the CSP plant and the financial assumptions stays the same. The default SAM financials in SAM 2020.11.29 were used. As of 2021, the ITC which is a key financial incentive for large solar projects, has been extended for commercial solar projects starting construction up to December 31, 2023 (DOE EERE, 2021b). We used the 26% ITC, assuming the CSP projects modeled in Table 6 start construction in 2021 or 2022 (SEIA, 2021). The ITC is currently expected to decrease to 10% after 2023 (SEIA, 2021). As seen in Table 6, the 26% ITC benefit significantly impacts the LCOE; for example, in Tucson, Arizona, in the default cost case, the LCOE drops by 20.2% with the ITC applied. We assumed any CSP project starting construction in 2021 and 2022 uses the full ITC.

As shown in Table 6, the change in potential installed cost for the heliostat field of approximately 1.1 Mm^2 has significant impact on the LCOE. At Location 1 (Tucson, Arizona), with the ITC applied, the reductions in heliostat field costs from $\$140/m^2$ to $127/m^2$ and $96/m^2$ in the Commercial and Advanced cases could lead to reductions in LCOE of 3% and 10% respectively. For Location 2 (Daggett, California), which has slightly higher DNI than Tucson, Arizona, changing the costs from the default $\$140/m^2$ for the heliostats to $\$127/m^2$ and $\$96/m^2$ has almost the same LCOE reductions as Arizona.

7 Discussion

Our analysis used DFMA as the main tool to estimate the manufacturing costs associated with the solar field components of two heliostat designs: the Stellio by sbp and the SunRing by Solar Dynamics. The flexibility and strength of DFMA comes from allowing users to create their own components and assemblies. In the case of the Stellio and the SunRing heliostats, most of the metal parts could be modeled within the tool. Our analysis follows the methodology used in a similar study NREL undertook for a modern heliostat design (Turchi and Heath, 2013), and more recently, the parabolic trough cost update (Kurup et al., 2021).

The DFMA analysis highlighted components and processes that benefit from large-volume production. We applied this tactic generally to components that required tooling costs that could be amortized over the increasing volume of production. For example, the stamped boomerang plate cost in the Stellio dropped from $1,000 to $6 per part when production was increased from 15 to 15,000 parts (raw material cost was unchanged). This production-volume effect is dramatically less for items available from stock suppliers. Conversely, the cost of a thinner and simpler plate within the boomerang that is laser-cut will not decrease significantly in cost with required quantity; this is because the material cost already represents more than 85% of the total part cost. The increase in manufacturing volume will benefit the setup times, batch sizes, and the move to increased automation but will reduce the part's overall cost by a few cents even at 500,000 parts.

The DFMA analysis we performed can be considered a "should-cost" assessment; that is, it answers the question, what should a component cost when based solely on material and manufacturing steps? The next level of sophistication using DFMA would be to examine "product costing" and "product simplification." In this type of investigation, researchers would study an overall design that employs alternative manufacturing processes, materials, and techniques; the objective would be to reduce part count and material content (Boothroyd Dewhurst Inc., 2020). These progressive steps could significantly cut the overall cost of systems. For example, in more than 500 surveys of its industrial users, DFMA developer Boothroyd Dewhurst (2015) found companies could save on average 30%–50% of the final product cost.

DFMA is well suited for our analysis of heliostat costs; the software gives a detailed snapshot in time even though it has some limitations. The detailed databases in the 2020 DFMA tool have cost data for a range of manufacturing processes (e.g., injection molding, stamping) and machining steps (e.g., machining material); however, the cost of materials is left to the user's discretion. For our analysis, we used the default U.S. labor and material costs. For our analysis, the raw material cost of U.S. low-carbon steel plate in DFMA was $0.64/lb in 2020 (Boothroyd Dewhurst Inc., 2020). Both the Stellio and the SunRing use significant quantities of steel structures, and the price volatility of steel in the global market would affect the raw material price. For example, outside of normal steel prices from 2010 through 2020, which only had a standard deviation of 9%, the raw price of low-carbon steel increased 235% between January and August of 2021 (U.S. BLS, 2021). The DFMA tool does not track commodity costs, so care must be taken to apply current raw material costs for an analysis. We used the 2020 values in the U.S. databases for the materials.

The steel price, which is based on region and time, will have a notable impact on total CAPEX for a heliostat field. The estimated Stellio and SunRing installed heliostat field CAPEX was found to be $137.29 million and $106.95 million respectively. If the 253% increase in steel prices in 2021 is used, the Stellio and SunRing fields increase by $38.4 million and $26.4 million respectively (U.S. BLS, 2021). This is because of the heavy use of steel in both designs. We used the 2020 steel prices in DFMA, as these can be considered to be closer to the normal costs for CSP developers.

As mentioned, the limitations of SAM modeling and the LCOE estimates are tied to the modeling of the specific sbp and SunRing heliostats. It is important to note the Commercial and Advanced scenarios modeled in Table 5 and Table 6 do not accurately consider the specific shape of the Stellio pentagonal heliostat or the performance of the SunRing heliostats. While heliostat performance can be modeled in SAM, pentagonal heliostats, for example, cannot be modeled. The LCOEs in Table 6 assume the heliostat performance for the Stellio and SunRing equal the current default heliostat performance of the 144.4 m^2 heliostats. The optical performance and modeling will be different for a pentagonal heliostat of 48.5 m^2 and for a smaller rectangular heliostat of 27 m^2. The optical performance modeling of the Stellio and SunRing are beyond the scope of this work. The optical performance of the Stellio would be expected to exceed that of the SunRing design. Therefore, we recommend future work consider the performance of heliostats be added to SAM and that the heliostat developers' estimates of heliostat performance be vetted before they are included in SAM.

7.1 Stellio Estimates

Stellio's installed costs were most sensitive to purchased component costs, such as costs for mirrors, control systems, and linear actuators, according to our analysis. Conversely the cost of raw steel had less effect. If the cost of the purchased components increased by 10%, the total field cost increased by $6.07 million. Yet if the cost of steel increased by 10%, the total field cost increased by $2.51 million. Mirrors had the highest sensitively, as they were 19% of the total heliostat cost. The linear actuators and control systems were the next two most costly components at 15% each. Even though the price of steel was less of a driver, sufficient manufacturing volumes must be achieved for the manufactured components. Accordingly, one must be aware of fluctuations in relevant commodities markets to track system cost over time.

7.2 SunRing Estimates

Our analysis found that the SunRing's installed costs were more sensitive to purchased components than manufactured components. In the case of the SunRing, a 10% increase of all the purchased parts drove our modeled field cost up $6.63 million. The largest drivers in this category were the mirrors and actuators, which together comprised over 30% of the total heliostat cost. The small amount of steel in the SunRing heliostat design means the field would increase only $1.72 million, for a 10% increase of steel costs. The high-volume manufacturing techniques employed, such as stamping, make this design significantly more effective at high-production volumes. Given the purchase of components are such a large lever on the cost of this design, accurate vendor quotations are paramount to correctly estimating its cost.

8 Conclusions

The aim of this project and detailed bottom-up modeling of two heliostat designs—one considered commercial, and one considered advanced and developing—was to determine the potential installed cost ($/m^2) for large solar fields of 22,239 and 40,000 heliostats.[3] In doing so, the analysis would help understand the state of the market. This aim has been successfully achieved.

Through DFMA modeling as part of detailed modeling, the estimated installed cost of the commercial sbp Stellio heliostat was found to be $127/m^2 and the installed cost of the advanced Solar Dynamics SunRing heliostat was found to be $96/m^2. Discussions with sbp and Solar Dynamics highlight that our analysis for each specific designs is within ±10% of the developer's own estimates for bids and projects.

As highlighted in Table 6 (page 23), the reduction of the estimated installed cost of a heliostat had significant impacts on the CAPEX of the field and the overall plant costs. This cost reduction then can reduce the LCOE of the plant and system. Reductions in the Commercial and Advanced cost cases from the current SAM default could reduce the overall heliostat installed field CAPEX by 9.3% and 31.5% respectively.

[3] The *performance* of the two designs was *not* modeled.

References

Acwa Power, 2021. Redstone CSP IPP [WWW Document]. Acwa Power. URL https://acwapower.com/en/projects/redstone-csp-ipp/ (accessed 9.16.21).

Akar, S., Augustine, C.R., Kurup, P., Mann, M.K., 2018. Global value chain and manufacturing analysis on geothermal power plant turbines (No. NREL/TP-6A20-71128). National Renewable Energy Lab (NREL), Golden, CO.

Balz, M., Göcke, V., Keck, T., von Reeken, F., Weinrebe, G., Wöhrbach, M., 2016. Stellio – development, construction and testing of a smart heliostat. Presented at the SOLARPACES 2015: International Conference on Concentrating Solar Power and Chemical Energy Systems, Cape Town, South Africa, p. 020002. https://doi.org/10.1063/1.4949026

BLS, 2020. May 2020 OEWS State Occupational Employment and Wage Estimates - Arizona [WWW Document]. Bur. Labor Stat. URL https://www.bls.gov/oes/2020/may/oes_az.htm#47-0000 (accessed 9.29.21).

Boothroyd Dewhurst Inc., 2020. Design for Manufacture and Assembly (DFMA) Product Costing and Simplification [WWW Document]. URL https://www.dfma.com/software/dfma.asp (accessed 9.20.21).

Boothroyd Dewhurst Inc., 2015. DFMA Webinars - Learn How Industry Wee U.|S. 500 Manufacturers Reduce Cost [WWW Document]. URL http://www.dfma.com/news/webdnld.htm (accessed 9.17.15).

Business Wire, 2021. EIG-Owned Cerro Dominador Inaugurates Concentrated Solar Power (CSP) Plant in Chile [WWW Document]. Bus. Wire. URL https://www.businesswire.com/news/home/20210608005202/en/EIG-Owned-Cerro-Dominador-Inaugurates-Concentrated-Solar-Power-CSP-Plant-in-Chile (accessed 7.6.21).

Chamberlain, K., 2019. Noor III Concentrated Solar power tower seen as “tipping point” for financing costs [WWW Document]. HELIOSCSP. URL https://helioscsp.com/noor-iii-concentrated-solar-power-tower-seen-as-tipping-point-for-financing-costs/ (accessed 7.6.21).

CSP Focus, 2020. Hami 50 MW CSP Project [WWW Document]. URL http://www.cspfocus.cn/en/study/detail_66.htm (accessed 9.16.21).

Dersch, J., Dieckmann, S., Hennecke, K., Pitz-Paal, R., Krüger, D., Ralon, P., 2019. LCOE Reduction Potential of Parabolic Trough and Solar Tower Technology in G20 Countries until 2030.

DOE EERE, 2021a. Generation 3 Concentrating Solar Power Systems (Gen3 CSP) Phase 3 Project Selection [WWW Document]. Energy.gov. URL https://www.energy.gov/eere/solar/generation-3-concentrating-solar-power-systems-gen3-csp-phase-3-project-selection (accessed 9.29.21).

DOE EERE, 2021b. Guide to the Federal Investment Tax Credit for Commercial Solar Photovoltaics.

IRENA, 2016. The Power To Change: Solar And Wind Cost Reduction Potential To 2025. International Renewable Energy Agency.

Kattke, K., 2019. The Drop-In, Ring-of-Power Heliostat.

Keck, T., Balz, M., Göcke, V., von Reeken, F., Gross, F., Landman, W., Collado, J., Salas, J., Gracia, J., Iriondo, J., Eizaguirre, I., Sun, D., 2019. Hami – The first Stellio solar field. Presented at the SOLARPACES 2018: International Conference on Concentrating Solar

Power and Chemical Energy Systems, Casablanca, Morocco, p. 030029. https://doi.org/10.1063/1.5117541
Kolb, G.J., Ho, C.K., Mancini, T.R., Gary, J.A., 2011. Power Tower Technology Roadmap and Cost Reduction Plan (Technical Report No. SAND2011-2419). Sandia National Laboratories, Albuquerque, NM.
Kolb, G.J., Jones, S.A., Donnelly, M.W., Gorman, D., Thomas, R., Davenport, R., Lumia, R., 2007. Heliostat Cost Reduction Study (Technical Report No. SAND2007-3293). Sandia National Laboratories, Albuquerque, NM.
Kraemer, S., 2019. Morocco's Ourazazate Noor III CSP Tower Exceeds Performance Targets [WWW Document]. SolarPACES. URL https://www.solarpaces.org/moroccos-ourazazate-noor-iii-csp-tower-exceeds-performance-targets/ (accessed 9.13.21).
Kraemer, S., 2018. Morocco's Noor III Solar Tower CSP to Deliver Power by October [WWW Document]. SolarPACES. URL https://www.solarpaces.org/moroccos-noor-iii-solar-tower-csp-deliver-power-october/ (accessed 9.13.21).
Kurup, P., Glynn, S., Akar, S., 2021. Manufacturing Cost Analysis of Advanced Parabolic Trough Collector: Preprint, in: AIP Conference Proceedings. Presented at the SolarPACES 2020: International Conference on Concentrating Solar Power and Chemical Energy Systems, NREL, Albuquerque, New Mexico.
Kurup, P., Remo, T., Jenne, D.S., Cotrell, J., O'Connor, P., 2018. Analysis of Supply Chains and Advanced Manufacturing of Small Hydropower (No. NREL/TP-6A20-71511). National Renewable Energy Laboratory (NREL), Golden, CO.
Kurup, P., Turchi, C., 2015. Parabolic Trough Collector Cost Update for the System Advisor Model (SAM) (No. NREL/TP-6A20-65228). NREL.
Lilliestam, J., Pitz-Paal, R., 2018. Concentrating solar power for less than USD 0.07 per kWh: finally the breakthrough? Renew. Energy Focus 26, 17–21. https://doi.org/10.1016/j.ref.2018.06.002
Mayyas, A., Mann, M., 2019. Manufacturing competitiveness analysis for hydrogen refueling stations. Int. J. Hydrog. Energy 44, 9121–9142. https://doi.org/10.1016/j.ijhydene.2019.02.135
Mehos, M., Turchi, C., Jorgenson, J., Denholm, P., Ho, C., Armijo, K., 2016. On the Path to SunShot: Advancing Concentrating Solar Power Technology, Performance, and Dispatchability (No. NREL/TP-5500-65688). EERE Publication and Product Library.
Mehos, M., Turchi, C., Vidal, J., Wagner, M., Ma, Z., 2017. Concentrating Solar Power Gen3 Demonstration Roadmap (Technical Report No. NREL/TP-5500-67464). National Renewable Energy Laboratory, Golden, CO. https://doi.org/10.2172/1338899
Murphy, C., Sun, Y., Cole, W.J., Maclaurin, G.J., Mehos, M.S., Turchi, C.S., 2019. The Potential Role of Concentrating Solar Power within the Context of DOE's 2030 Solar Cost Targets (No. NREL/TP--6A20-71912, 1491726). Golden, CO. https://doi.org/10.2172/1491726
NREL, 2021. 2021 Annual Technology Baseline - Electricity - Concentrating Solar Power [WWW Document]. URL https://atb.nrel.gov/electricity/2021/concentrating_solar_power (accessed 8.13.21).
NREL, 2020a. 2020 Annual Technology Baseline [WWW Document]. URL https://atb.nrel.gov/electricity/2020/index.php?t=sc (accessed 7.6.21).
NREL, 2020b. Download - System Advisor Model (SAM) [WWW Document]. URL https://sam.nrel.gov/download.html (accessed 9.15.20).

REN21, 2021. Renewables 2021 Global Status Report (No. ISBN 978-3-948393-03-8). Renewable Energy Network for the 21st Century, Paris, France.
SEIA, 2021. Solar Investment Tax Credit (ITC) [WWW Document]. Sol. Energy Ind. Assoc. URL https://www.seia.org/initiatives/solar-investment-tax-credit-itc (accessed 9.19.21).
Sener, 2019. Central Receiver Plant Noor Ouarzazate III [WWW Document]. Sener. URL https://www.energy.sener/project/central-receiver-plant-nooro-iii (accessed 7.6.21).
Shultz, A., 2021. SETO Introduction and Overview of the Gen3 CSP Program.
SolarPACES, 2021. CEEC Hami - 50MW Tower CSP Project [WWW Document]. URL https://solarpaces.nrel.gov/project/ceec-hami-50mw-tower (accessed 9.16.21).
SolarPACES, 2020. CSP Projects Around the World [WWW Document]. Solarpaces. URL https://www.solarpaces.org/csp-technologies/csp-projects-around-the-world/ (accessed 3.23.20).
SolarPACES, 2019. DEWA CSP Trough Project [WWW Document]. URL https://solarpaces.nrel.gov/dewa-csp-trough-project (accessed 3.23.20).
SQM, 2018. Thermo-Solar Salts [WWW Document]. SQM. URL https://www.sqm.com/en/producto/sales-termo-solares/ (accessed 7.6.21).
Tilley, D., Kelly, B., Burkholder, F., 2014. Baseload Nitrate Salt Central Receiver Power Plant Design. Abengoa Solar LLC, Lakewood, CO (United States).
Turchi, C., 2010. Parabolic Trough Reference Plant for Cost Modelling with the Solar Advisor Model (SAM) (No. NREL/TP-550-47605). NREL, Golden, CO.
Turchi, C., Boyd, M., Kesseli, D., Kurup, P., Mehos, M., Neises, T., Sharan, P., Wagner, M., Wendelin, T., 2019. CSP Systems Analysis - Final Project Report (No. NREL/TP-5500-72856). National Renewable Energy Laboratory, Golden, CO.
Turchi, C., Heath, G., 2013. Molten salt power tower cost model for the system advisor model (SAM) (No. NREL/TP-5500-57625). NREL, Golden, CO.
Turchi, C.S., Kurup, P., Akar, S., Flores, F., 2015. Domestic Material Content in Molten-Salt Concentrating Solar Plants (Technical Report No. NREL/TP-5500-64429). National Renewable Energy Laboratory.
Turchi, C.S., Stekli, J., Bueno, P.C., 2017. 11 - Concentrating Solar Power, in: Brun, K., Friedman, P., Dennis, R. (Eds.), Fundamentals and Applications of Supercritical Carbon Dioxide (SCO_2) Based Power Cycles. Woodhead Publishing, pp. 269–292. https://doi.org/10.1016/B978-0-08-100804-1.00011-6
U.S. BLS, 2021. U.S. Bureau of Labor Statistics, Producer Price Index by Commodity: Metals and Metal Products: Cold Rolled Steel Sheet and Strip , retrieved from FRED, Federal Reserve Bank of St. Louis; https://fred.stlouisfed.org/series/WPU101707, . (No. [WPU101707]).
Van Geet, O., Fu, R., Horowitz, K., Kurup, P., MacAlpine, S., Silverman, T.J., 2018. Analyzing the Energy Performance, Wind Loading, and Costs of Photovoltaic Slat Modules on Commercial Rooftops (No. NREL/TP--7A40-70681). NREL, Golden, CO. https://doi.org/10.2172/1421779